Jpn. J. Appl. Phys. Vol. 41 (2002) pp. 6595–6600
Part 1, No. 11A, November 2002

Fabrication of a Piezoelectric Impact Hammer and Its Application to the *In-situ* Nondestructive Evaluation of Concrete

J.-H. TONG[1]*, T.-T. WU[2] and C.-K. LEE[2]

[1]*Department of Computer Science & Information Engineering, Hungkuang Institute of Technology, Taichung Shien, Taiwan 433, R.O.C.*
[2]*Institute of Applied Mechanics, National Taiwan University, Taipei, Taiwan 106, R.O.C.*

(Received March 25, 2002; accepted for publication July 1, 2002)

In this paper, a piezoelectric impact hammer is designed and fabricated for generating stable repeated impact elastic waves and further for *in-situ* wave velocity measurements of concrete specimens. The piezoelectric impact hammer consists of a stacked multilayer PZT, a flying head system with an on-line load cell embedded and a holding fixture. To measure the longitudinal or Rayleigh waves of a concrete specimen, two horizontally polarized conical transducers are utilized to receive the elastic waves generated by the piezoelectric impact hammer. Due to the stable impact generation of the piezoelectric impact hammer, the experimental results showed that the accuracy of the wave velocity measurement was enhanced significantly through the signal averaging. Since the impact time origin of the newly designed impact hammer can be determined accurately, it was utilized to measure the depth of a normal surface-breaking crack in a concrete specimen, and the result is very accurate. We note that the results of this study offer a precise and convenient way of measuring *in-situ* elastic properties and/or crack depth of concrete specimens. [DOI: 10.1143/JJAP.41.6595]

KEYWORDS: piezoelectric material, impact hammer, concrete, elastic wave

1. Introduction

In the field of nondestructive evaluation of concrete, the ultrasonic wave velocity is usually measured and utilized to predict or correlate the strength of concrete.[1,2] In the measurement, two low-frequency ultrasonic transducers with relatively large aperture are usually employed. Depending on the *in-situ* concrete structure geometry, different transducer arrangements were suggested. In addition to the ultrasonic method, various methods based on the point-source/point-receiver technique that utilize transient elastic wave response have been proposed, and several successful applications have been reported.[3–6] In those methods that are based on the transient elastic wave responses, steel ball impact sources and conical PZT displacement sensors are usually adopted.

Recently, Wu and Fang[7] proposed a method for determining the elastic wave velocities of a concrete specimen using transient elastic waves. In the method, the Rayleigh wave velocity was determined based on the cross correlation of the surface responses and the longitudinal wave velocity was determined by measuring the wavefront arrival of the skimming longitudinal wave. The longitudinal wavefront can be identified from the horizontally polarized surface responses directly. In the above-mentioned method, a hand-held steel ball impactor was used to generate the elastic waves. However, due to the difficulty in controlling the impact force and the time origin, the averaging method, which is commonly adopted in ultrasonics to improve the signal-to-noise ratio, cannot be applied. In addition, due to the lack of the information of the impact time origin, the application of the point-source/point-receiver technique to the imaging of a crack in concrete has some limitations.

To reduce the noise level in the stress wave measurements in concrete, Popvics *et al.*[8] used a DC-powered solenoid with a spring-loaded steel shaft as the stress wave source and thus reduced the noise level by averaging the repeated impact signals. However, a quantitative report of the noise level reduction has not been included. In addition, the time origin of the impact is still hard to find. The waveguide concept has been applied to design a high-speed piezoelectric-driven system for application in the printer industry by Chang and Wang.[9,10] Later, the mechanism was improved by Wu and Lee,[11] which included an on-line load cell to detect the impact force for microimpact applications such as the study of the mechanical properties of amorphous carbon under high-rate indentation. The high-speed piezoelectric hammer has also been applied recently to the structural modal testing of a small metallic structure to give precise impact timing and positioning by Lee *et al.*[12] To the best of our knowledge, the application of the waveguide-based piezoelectric hammer to the nondestructive evaluation (NDE) of concrete structure has not been reported.

In this study, a piezoelectric impact hammer is designed and fabricated for applications in the nondestructive evaluation of concrete structures. To determine the accurate time origin of the impact, a tiny piezoelectric sensor is embedded in the flying head of the impact hammer to detect the impact signal. A gated circuit is also designed to gate the impact signal and send a synchronous pulse as the trigger time reference. With the on-line sensor, the impact time origin resolution can be controlled in the range of sub-microsecond. Calibration experiments on the precise determination of the time origin of the impactor were conducted to determine the true time origin of the impact hammer system. To demonstrate the accuracy of the newly fabricated impact device, measurements of the longitudinal and Rayleigh wave velocities of a concrete specimen were conducted. In addition, measurement of the depth of a surface-breaking crack in a concrete specimen was also conducted.

2. Piezoelectric Impact Hammer System for Concrete Testing

Piezoelectric material is known to have the ability to generate large force but with very little deformation. In order

*Correspondence author. E-mail address: jhtong@sunrise.hkc.edu.tw
Postal address: No. 34, Chung-Chie Rd., Shalu, Taichung Shien 433, Taiwan, R.O.C.

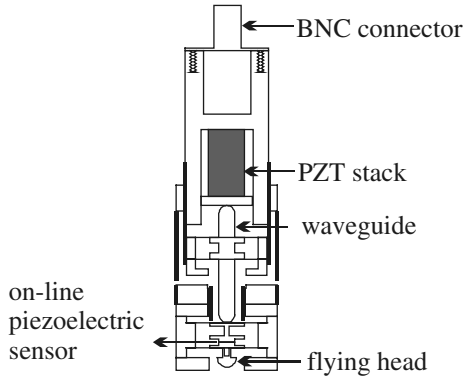

Fig. 1. Piezoelectric impact hammer.

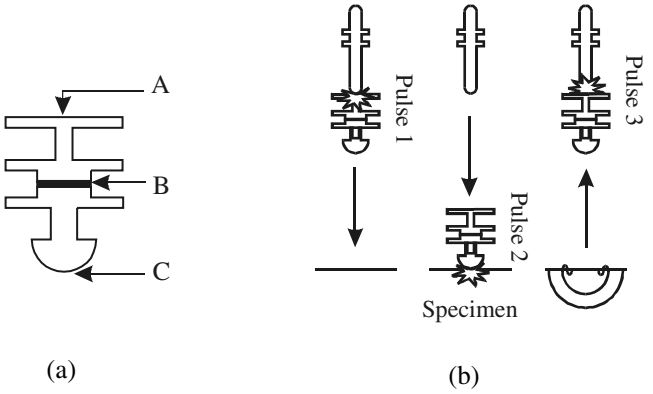

Fig. 2. (a) Flying head system (b) Three impact stages.

to transform the blocking force of the piezoelectric material into a free fly motion, the waveguide concept[9] is adopted in this paper. Figure 1 shows the basic design of a piezoelectric impact hammer for generating elastic waves in concrete structures. The hammer is composed of three major parts, the PZT stack, the waveguide, and the assemblage of the flying head. The cross section of the PZT rectangular stack is 10 mm $\times$ 10 mm and the length is 20 mm. The maximum generation force of the PZT stack is 3500 N, while its maximum displacement is 18.4 μm and the corresponding resonant frequency is 69 kHz. The diameter of the cylindrical waveguide is 5 mm and the length is 37 mm. The flying head consists of a semisphere impactor of 3 mm radius and an on-line piezoelectric sensor. The sensor is a tiny PZT disk of approximately 2 mm in diameter.

It is worth noting that the capacitance of the PZT stack is as high as 5.4 μF and the driving voltage is 150 V; therefore, to generate a sufficiently large power to drive the impact hammer, a high voltage pulse generator is needed. In this study, a laborat-built 150 V voltage pulse generator, which is composed of a capacitor bank and an N-channel metal oxide semiconductor field-effect semiconductor (MOSFET), is used in this study.

In addition, a gated circuit was fabricated to gate the impact signal from the on-line piezoelectric sensor and to send a trigger signal synchronous with the impact time origin.

3. Calibration of the Impact Hammer System

The time origin of an impact induced by the piezoelectric hammer can be estimated from the triggering signal of the hammer and the fixed flying time from the waveguide to the testing surface. For a flat sample surface and a relatively small impactor, the above estimation method results in a resolution in the microsecond range. However, this is not true for the case of testing in a concrete specimen. The surface of a concrete specimen is uneven as compared with that of a metal surface, in general. Therefore, the distance the flying head flies from the waveguide to the surface of the specimen is not a constant. The deviation of the flying distance results in deviation in the flying time estimation. In addition, there is also deviation in the speed of the flying head for different triggers, which will also cause errors in the flying time estimation. For example, the flying time variance is about 20 μs for testing on a concrete specimen using the current fabricated piezoelectric hammer. This variation is

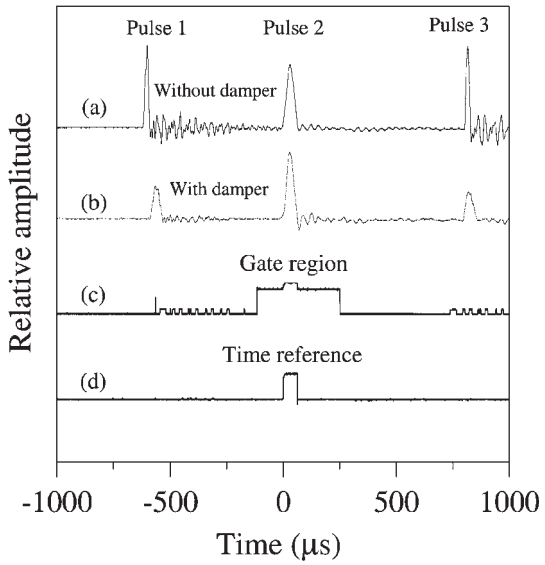

Fig. 3. Signal from the on-line piezoelectric sensor (without damper, trace a: with damper, trace b: gated region, trace c: and the time reference, trace d).

unacceptable for measurement of elastic wave velocity of concrete.

To overcome the above-mentioned difficulties, an on-line piezoelectric sensor was embedded in the flying head system to determine the precise time reference and/or time origin of the impact at the specimen surface. Figure 2(a) shows the design structure of the flying head system and the piezoelectric sensor is located at point B. Figure 2(b) shows the three impact stages of the flying head system that will occur in a test. The trace (a) shown in Fig. 3 is the signal detected by the on-line piezoelectric sensor for a particular impact on a concrete specimen. Three separate pulses corresponding to the three impact stages are found in the signal. Pulse 1 is the first signal received by the on-line sensor for wave transmitting from the waveguide [point A, Fig. 2(a)] to the sensor (point B). Pulse 2 denotes the back propagation wave induced by the impact of the flying head on the testing surface (point C) and reflected back to the sensor (point B). Pulse 3 is generated by the impact between the bounced back flying head and the waveguide. In addition to the three main pulses in trace (a) of Fig. 3, there are many ripples induced by the waves bouncing back and forth inside the flying head. To minimize these unwanted reflections, we adhered a

viscous tape to the back surface of the flying head system (point A). As shown in trace (b) of Fig. 3, we note that the reflections between point A and point B, i.e., the ripples after pulse 1, significantly reduced.

The time reference of this impact device can thus be deduced from the true impact signal, pulse 2, which is induced by the flying head hitting the specimen. A gated circuit was designed to gate pulse 2 (trace c) and to send a synchronous pulse out as the time reference of the measuring system (trace d of Fig. 3). With this circuit, the accuracy of time reference of the impact can be improved to the range of sub-microsecond.

The time reference mentioned above was utilized to average the repeated signals to enhance the S/N ratio. However, some applications of the impact hammer, such as crack depth evaluation, require not only an accurate time reference but also the true impact time origin. To determine the impact time origin, a calibration experiment on a steel block was conducted. As shown in Fig. 4, a 9 V battery was used as the voltage source to give the impact time origin. As the flying head hits the steel surface, a circuit loop is formed and this gives a step signal with a very short rise time (about 0.02 μs). The experimental result (Fig. 5) showed that the time delay between the time reference and the 9 V step signal (the true impact time origin) is about 7.2 μs.

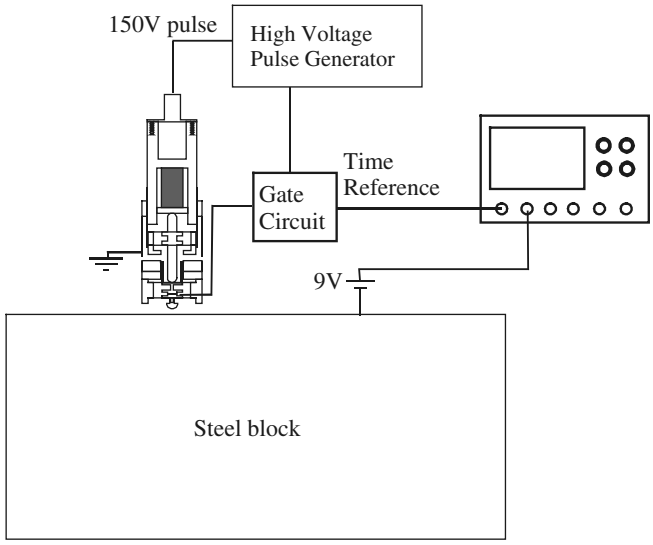

Fig. 4. Arrangement of the calibration experiment.

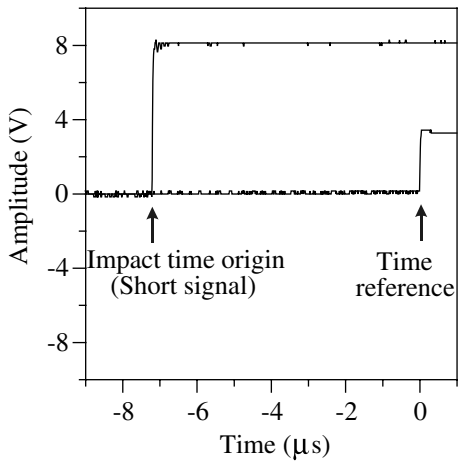

Fig. 5. Experimental result of the calibration experiment.

4. Principle of *in-situ* Wave Velocity Measurements

4.1 Longitudinal wave velocity measurement

An analysis carried out by Wu and Fang[7] has shown that for elastic wave generation by a point source in a half space, the amplitude of the tangential component of the skimming longitudinal wave is four to five times larger than that of the normal component. In addition, it gives a much clearer displacement jump at the wavefront arrival. For this reason, a pair of horizontal polarized conical PZT transducers were employed to measure the wavefront arrival of the surface-skimming longitudinal wave.

4.2 Rayleigh wave velocity measurement

In the measurement of Rayleigh wave velocity using the transient elastic wave, the method proposed by Wu *et al.*[6] was adopted. In the method, the relative positions of an impact source and two receivers (S_1 and S_2) are shown in Fig. 6. The distance between the source and the first receiver S_1 is r_1, and the distance between the first receiver and the second receiver S_2 is d. In order to utilize the cross correlation method to determine the Rayleigh wave transit time between the first receiver and the second receiver, it is required that the wave responses received at these two receivers must be dominated by the Rayleigh waves. Therefore the distance r_1 must be sufficiently large to ensure that the Rayleigh wave carries most of the energy. Let $h_1(t)$ and $h_2(t)$ be the signals recorded at S_1 and S_2, respectively. The cross correlation function of these two signals is defined as

$$z(t) = \int_{-\infty}^{\infty} h_1(\tau)h_2(t+\tau)d\tau \qquad (1)$$

If the signals $h_1(t)$ and $h_2(t)$ are similar with a time delay Δt, the maximum of $z(t)$ occurs at Δt. In other words, the time delay between $h_1(t)$ and $h_2(t)$ can be determined by finding the corresponding time at which $z(t)$ is maximum.

5. Experimental Verification

In the measurements of *in-situ* wave velocities of concrete specimens, instead of finding the time origin of an impact source, two transducers to measure the time delay between the wavefront arrivals received at the two different positions can be used. The source and the receivers are located on the same straight line. Since the distance between the receivers is known, the wave velocity can be obtained without knowing the time origin of the impact source. However, the piezoelectric impact hammer does give us stable impact with repeatable impact force and constant time reference. Therefore, the signal-to-noise ratio for a wave signal in concrete can be improved significantly by the averaging method. In this study, two laborat-built horizontally

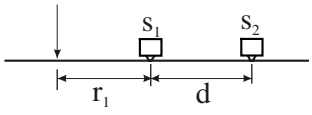

Fig. 6. Relative positions of the impact source and receivers.

polarized conical transducers were utilized to measure the tangential component of the surface displacement signals. The received voltage signal from the conical transducer was amplified by a preamplifier and recorded by a 100 MHz digital oscilloscope (LeCroy 9314L). We note that to minimize the electric noise, the preamplifier must be embedded in the transducer assembly.

The dimensions of the concrete specimen used in this study are 60 cm × 80 cm in width and length and 30 cm in height. The water-to-cement (W/C) ratio of the concrete specimen is 0.58.

5.1 Longitudinal wave measurement

In determining the longitudinal wavefront arrival using a hand-held impactor,[7] to enhance the resolution of the delay time measurement, the recorded signal was enlarged and processed by a linear phase finite impulse response filter. Shown in Fig. 7 are the measured signals by utilizing the two horizontally polarized conical transducers. The distance from the impact source to the first receiver was kept $r_1 =$ 7 cm. The distance between the first receiver and the second receiver was kept at a constant distance of 10 cm. The signals showed that there are a lot of noises riding on top of the elastic wave signals, and hence to determine the true arrival of the longitudinal wavefront, special care is needed to ensure a reliable measurement. Although the hand held impactor method can give a measurement of the longitudinal wavefront arrival with reasonable accuracy, it is time-consuming and is not practical for *in-situ* measurement.

Figure 8 shows the results of the longitudinal wavefront measurements using the newly fabricated piezoelectric hammer with 40 times averaging. The results showed that the signal-to-noise ratio was improved significantly, and therefore, the wavefront arrivals can be detected automatically by setting a common triggering level. Table I shows the results for four different measurements of the longitudinal wave velocities at the same location of the concrete specimen. The average longitudinal wave velocity is 3974 m/s and the standard deviation of the four measurements is 0.47%, which is very small for concrete applications.

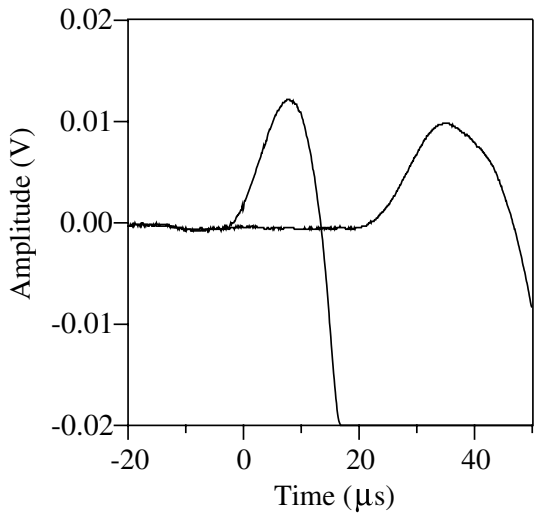

Fig. 8. Averaged (40 times) displacement signals of the longitudinal wave measurements.

Table I. Four different measurements of the longitudinal wave velocities at the same location of the concrete specimen.

	1st	2nd	3rd	4th	Average
Velocity	4000 m/s	3960 m/s	3960 m/s	3976 m/s	3974 m/s
Deviation	0.65%	−0.35%	−0.35%	0.05%	
Standard deviation = 0.47%					

5.2 Rayleigh wave measurement

Figures 9 and 10 show the Rayleigh wave signals generated by a hand-held impactor and the piezoelectric impact hammer (20 times averaging), respectively. Significant improvement of the signal-to-noise ratio has been achieved. To calculate the travel time delay between the two receivers, the signals after the peaks of the Rayleigh waves have been removed before conducting the cross correlation of the two signals. Table II shows the results for four different measurements of the Rayleigh wave velocities at the same location of the concrete specimen. The average Rayleigh wave velocity is 2178 m/s and the standard

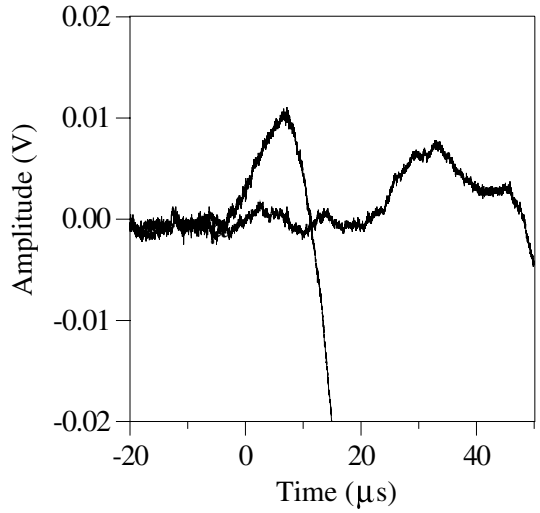

Fig. 7. Received displacement signals of the longitudinal wave measurement using a hand-held impactor.

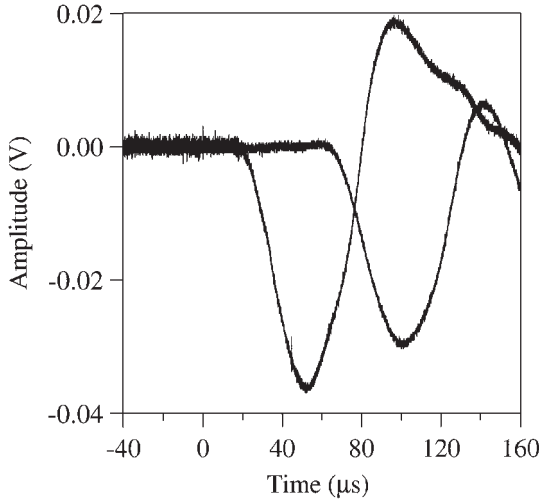

Fig. 9. Received displacement signals of the Rayleigh wave measurement using a hand-held impactor.

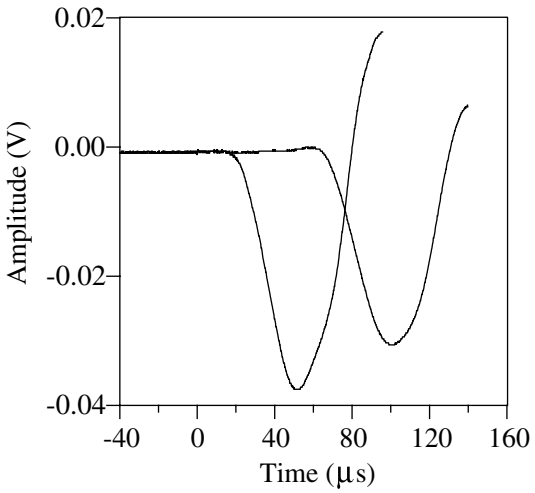

Fig. 10. Averaged (20 times) displacement signals of the Rayleigh wave measurement.

Table II. Four different measurements of the Rayleigh wave velocities at the same location of the concrete specimen.

	1st	2nd	3rd	4th	Average
Velocity	2140 m/s	2140 m/s	2137 m/s	2137 m/s	2139 m/s
Deviation	0.08%	0.08%	−0.08%	−0.08%	
Standard deviation = 0.08%					

deviation of the four measurements is 0.08%. The results showed that the Rayleigh wave velocity measurement using the newly designed piezoelectric impact hammer is accurately repeatable.

5.3 Crack depth measurement

Measurement of the size and geometry of a surface-breaking crack is important in the evaluation of an existing concrete structure. The presence of surface-breaking cracks in a concrete structure decreases its durability significantly. The position of a surface-breaking crack can easily be observed by the naked eye; however, the determination of the depth of the crack is not as trivial. In this subsection, we applied the piezoelectric hammer to measure the wavefront arrival of the diffracted longitudinal wave, and therefore, to evaluate the depth of a normal surface-breaking crack in a concrete specimen.

Figure 11 shows the setup of crack measurement in this study. The crack depth is 9 cm and the distance from the surface breaking to the source is $D_1 = 10$ cm and that from the surface break to the receiver is $D_2 = 10$ cm. As shown in Fig. 12, by using the newly fabricated piezoelectric impact

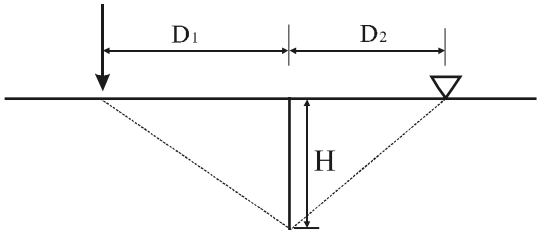

Fig. 11. Arrangement of the crack depth measurement.

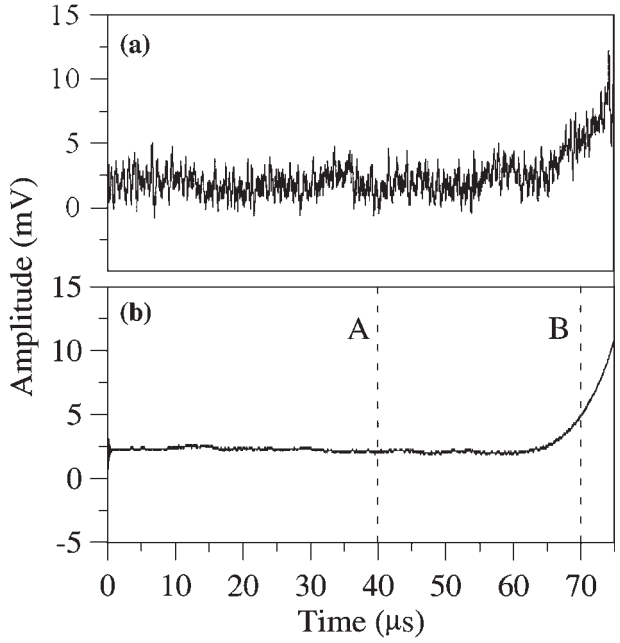

Fig. 12. Measured diffracted wave signals form a surface-breaking crack in concrete.

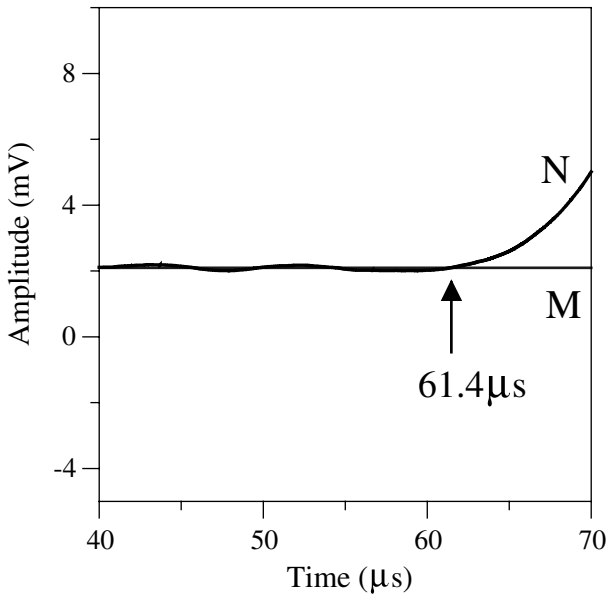

Fig. 13. Enlargement of part of the signal in Fig. 12.

source, the noises contained in the diffracted wave [Fig. 12(a)] can be reduced significantly with averaging of the repeated signals 20 times as shown in Fig. 12(b). Figure 13 shows enlargement of a segment of the signal from A to B in Fig. 12(b). To estimate the arrival time of the diffracted wave by the crack tip, the arrival signal N is dealt with moving average fitting and the undisturbed datum line M, which has certain DC offset caused by low frequency EM noise, is obtained by averaging the signal from 0 μs to 50 μs. Then, the traveling time of the first P-wave arrival can be determined as 68.6 μs, which is the summation of 61.4 μs, the time point at which line N is just crossing line M up, and 7.2 μs, the system delay. The P-wave velocity around the crack was measured to be 3974 m/s as mentioned in the

previous section, and hence the corresponding crack depth was calculated as 92.3 mm. The difference between the measured value (92.3 mm) and the real one (90.0 mm) may be result of the inhomogeneity of the concrete specimen. The P-wave velocity is measured on the surface of the specimen; however, it does not reflect the real value along the traveling path. In spite of this, the results show great potential for the new fabricated impact hammer to be applied in the NDT field of concrete structures.

6. Conclusions

In this study, a piezoelectric impact hammer has been designed for applications in the nondestructive evaluation of concrete structures. The accurate impact time origin has been determined by embedding a tiny piezoelectric sensor in the flying head. With the on-line sensor, the impact time origin resolution can be controlled in the range of sub-microsecond. Measurements of the longitudinal and Rayleigh wave velocities of a concrete specimen were conducted. Due to the stable impact generation of the piezoelectric impact hammer, the experimental results showed that the accuracy of the wave velocity measurement is enhanced significantly through signal averaging. The ability of the newly designed impact hammer to detect the accurate impact time origin has also been utilized to measure the depth of a normal surface-breaking crack in a concrete specimen, and an accurate result was obtained. We note that the results of this study offer a precise and convenient way of measuring *in-situ* elastic properties and/or crack depth of concrete specimens.

Acknowledgment

The authors thank the National Science Council of ROC for the financial support of this research through the grant NSC90-2735-E-241-002.

1) "Standard Test Method for Pulse Velocity Through Concrete," ASTMC597-71 (1979).
2) A. E. Ben-Zeitun: Int. J. Cement Comp. Light Weight Concrete **8** (1986) No. 1, 51.
3) N. J. Carino, M. Sansalone and N. N. Hsu: ACI J. Proc. **83** (1986) 199.
4) N. J. Carino and M. Sansalone: ACI Mater. J. **89** (1992) 296.
5) T.-T. Wu, J.-S. Fang and P.-L. Liu: J. Acoust. Soc. Am. **97** (1995) 1678.
6) T.-T. Wu, J.-S. Fang, G.-Y. Liu and M.-K. Kuo: J. Acoust. Soc. Am. **98** (1995) 2142.
7) T.-T. Wu and J.-S. Fang: J. Acoust. Soc. Am. **101** (1997) 330.
8) J. S. Popvics, W. Song, J. D. Achenbach, J. H. Lee and R. F. Andre: J. Eng. Mech. **124** (1998) 1346.
9) P. S. H. Chang and H. C. Wang: U.S. Patent 5046872 (1988).
10) P. S. H. Chang and H. C. Wang: Sens. Actuat. **24** (1990) 239.
11) T. W. Wu and C. K. Lee: J. Mater. Res. **9** (1994) 787.
12) C. K. Lee, C. T. Lin, C. C. Hsiao and W. C. Liaw: J. Guid. Control Dynam. **21** (1998) 692.